URSI - RCRS 2022, IIT (Indore), India, 1 - 4 December, 2022

Design of an Efficient GeSn Based Grating Coupler to excite Plasmon Waves in 3-20 μm MIR Range in GeSn/SiGeSn Structure on Si Platform

Bratati Mukhopadhya [(1)] and Prasanta Kumar Basu [(1)]
Institute of Radio Physics and Electronics, University of Calcutta,
92 Acharya Prafulla Chandra Road, Kolkata 700009, INDIA
bmrp@caluniv.ac.in pkbasu.rpe@ieee.org

Abstract

We describe in this paper the design of a GeSn alloy based planar grating to efficiently excite surface plasmon waves in a heavily doped GeSn layer replacing the usual metal conductor. The Ge_{1-x} Sn_x layer is grown on $Si_{1-y-z}Ge_ySn_z$ layer which may be grown on Si platform. The composition *x, y* and *z* are chosen to give rise to tensile, compressive and no strain in GeSn layer. The plasma frequency, real and imaginary parts of permittivity, etc., are calculated by using the modified Drude model developed by us. The optimized grating period and height for efficient coupling are calculated analytically.

1. Introduction

Plasmonic devices are attractive for feature size in the subwavelength range of the optical wave exciting surface plasmon (SP) waves. The strong light-matter interaction is exploited in sensing and other photonic applications [1-4]. Usually metal-insulator (semiconductor) structures with noble metals like Ag, Au etc. are used for the study of plasmonics. However, the excessive loss in metals, particularly in the IR and mid IR range (MIR), demands the use of heavily doped semiconductors like GaAs and InP [3], and Ge and/or alloy GeSn [5, 6] as their replacement. Ge or its alloy can be grown on Si platform to make the devices CMOS compatible [6, 7]. In the work reported in [6], the layer considered was Ge rich alloy which is an indirect gap material providing substantial loss.

The present paper describes a structure of Ge_{1-x} Sn_x based plasmonic system in which the surface plasmon (SP) waves propagate along a $Ge_{1-x}Sn_x$ layer grown on a Si_{1-y-z} Ge_ySn_z layer. The SP wave is excited by a coplanar GeSn grating upon which the EM wave in the range 3-20 μm is incident. The grating coupling is used instead of prism coupling to maintain planar geometry. The whole structure is grown on Si.

It is known that the two conduction band valleys in Ge or GeSn, the direct Γ valley and the indirect fourfold *L* valleys, change their positions with composition *x* and the free standing alloy starts becoming direct gap with $x > 0.08$. The supporting SiGeSn layer can produce tensile, compressive or no strain in GeSn by changing compositions *x*, *y* and *z*. Since electron mobility is quite large in Γ valley than in *L* valleys [8, 9], we have chosen the compositions to ensure that the population ratio f_Γ/f_L to be as large as possible. For heavy doping in GeSn, the population in the valleys obey Fermi statistics.

We first calculate the compositions to make GeSn a direct gap under strain and unstrained conditions and then calculate the electron population in the two valleys. A modified Drude model developed in [10] is then used to calculate the plasma frequency and the real and imaginary parts of the permittivity. The -ve values of real permittivity for doping density > $10^{20}/cm^{-3}$ ensures propagation of SP waves along the GeSn layer over the range 3-20 μm.

The design of GeSn planar grating follows next. We aim to optimize the height *h* and period *d* of the sinusoidal grating to couple the EM wave with the GeSn layer supporting propagating SP waves. An analytical method developed in [11] is employed for this purpose.

The structure, methods of determination of compositions and population and calculation of optimized values of *h* and *d* are presented in the following sections.

2. Structure

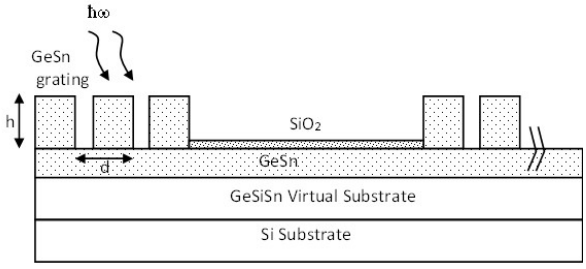

FIG. 1: Cross sectional diagram of grating coupled structure. The input grating is excited by EM wave of photon energy ħω and couples to GeSn layer along which SP waves propagate. An output coupler is used to convert SP waves.

A schematic cross sectional diagram of the structure used in the work is shown in Fig. 1. The GeSn grating couples

the incident EM wave of angular frequency ω, in the MIR range, to the GeSn layer to excite SP waves which propagate lengthwise and is detected by a similar output coupler. The GeSn alloy is grown on SiGeSn layer, which acts as a virtual substrate (VS). The thick VS layer in turn is grown on the Si substrate, so as to accommodate threading dislocations arising out of strain between the VS and Si substrate within a short distance near the SiGeSn-Si interface. Thus the GeSn layer becomes defect free. The thin SiO_2 layer on GeSn layer acts as the insulator.

The growth of the structure shown in Fig. 1, the design of which is undertaken in this paper by using mostly analytical techniques, is CMOS compatible. This type of structure has already been grown in [6]. Further details of growth processes of CMOS compatible photonic structures using Group IV semiconductor alloys may be found in [7].

3. Method of Calculation

We first find out the compositions *x, y* and *z* so that the GeSn layer remains always direct gap under both strained and unstrained conditions. Furthermore, it is aimed to make the separation of Γ and *L* valleys as large as possible to populate the direct valley and to maximize the electron mobility to reduce the loss of SP waves. The lattice constants and energies of conduction band valleys are obtained by using expressions given in [8, 9] with bowing parameters.

The compositions of GeSn and SiGeSn layers are determined under strain and no strain conditions restricting the strain below 2%.

The population densities in the two valleys are obtained by solving two equations involving two Fermi integrals as mentioned in our earlier work [10]. The corresponding values of mobilities are then obtained from our theory described in [8].

The next step is to calculate the plasma frequency and the real and imaginary parts of permittivity, ε_1 and ε_2, respectively by using the modified Drude model of ours [10].

The permittivity can be written as [10]

$$\varepsilon = \varepsilon_s\varepsilon_0\left[1 - e^2\left(\frac{n_1}{m_1\left(\omega^2 + \frac{i\omega}{\tau_1}\right)} + \frac{n_2}{m_2\left(\omega^2 + \frac{i\omega}{\tau_2}\right)}\right)\right] \quad (1).$$

It is to be noted from Eq.(1) that only when $\omega\tau_1$ and $\omega\tau_2 \gg 1$, we may write for the permittivity as [10]

$$\varepsilon = \varepsilon_s\varepsilon_0\left[1 - \frac{\omega_p^2}{\omega^2}\right] \quad (2).$$

where the plasma frequency is given by

$$\omega_p^2 = \frac{ne^2}{\varepsilon_s\varepsilon_0}\left[\frac{n_1}{nm_1} + \frac{n_2}{nm_2}\right] = \frac{ne^2}{\varepsilon_s\varepsilon_0}\left[\frac{f_1}{m_1} + \frac{f_2}{m_2}\right] \quad (3).$$

and f_1 and f_2 denote, respectively, the fraction of electrons occupied by the valleys 1 and 2.

The second term within square brackets in Eq. (1), preceded by the –ve sign gives the carrier induced changes in the real and imaginary parts of the permittivity, which are expressed as

$$\Delta\varepsilon_r = \varepsilon_s\varepsilon_0\left[1 - e^2\left(\frac{n_1}{m_1\left(\omega^2 + \frac{i\omega}{\tau_1}\right)} + \frac{n_2}{m_2\left(\omega^2 + \frac{i\omega}{\tau_2}\right)}\right)\right] \quad (4).$$

$$\Delta\varepsilon_i = \varepsilon_s\varepsilon_0\left[1 - e^2\left(\frac{n_1}{m_1\left(\omega^2 + \frac{i\omega}{\tau_1}\right)} + \frac{n_2}{m_2\left(\omega^2 + \frac{i\omega}{\tau_2}\right)}\right)\right] \quad (5).$$

Finally the optimized height h and period d of the sinusoidal grating made of GeSn are obtained from the following two equations given by [11]

$$d_{opt} = \frac{\lambda}{n_{cov}\left(1 + \left(\beta_m + \beta_n/2\sqrt{3}\right)^2\right)} \quad (6).$$

$$h_{opt} = \frac{2d_{opt}}{\pi}\sqrt{\frac{n}{2(m^2 + n^2)}} \quad (7).$$

where the refractive n_{cov} of the cover medium is set to 3.9 (SiO_2). The complex permittivity is set as $\varepsilon = (n + im)^2$, $\beta_m = m/(m^2 + n^2)$ and $\beta_n = n/(m^2 + n^2)$.

4. Results and Discussions

We have considered both tensile and compressively strained as well as unstrained GeSn layers. Typical compositions obtained for the three cases are: unstrained: $Ge_{0.82}Sn_{0.12}$/ $Ge_{0.06}Si_{0.81}Sn_{0.13}$; < 1% compressively strained $Ge_{0.88}Sn_{0.12}$/ $Ge_{0.09}Si_{0.80}Sn_{0.11}$, and ~ 2% Compressively strained: $Ge_{0.88}Sn_{0.12}$/$Ge_{0.02}Si_{0.90}Sn_{0.08}$.

Fig. 2 displays the variation of the ratio of electron concentration f_L/f_Γ with doping concentration. As expected, the large density-of-states in the *L* valley makes the ratio

large for the unstrained case. With more compressive strain, the separation between the valleys increases and the direct Γ valley becomes more populated.

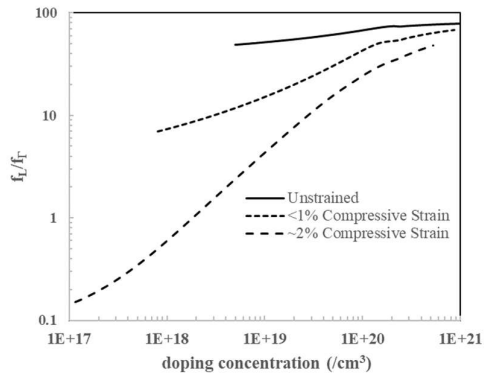

Fig 2: Ratio of electron population in the two valleys as a function of doping density in three different strain conditions.

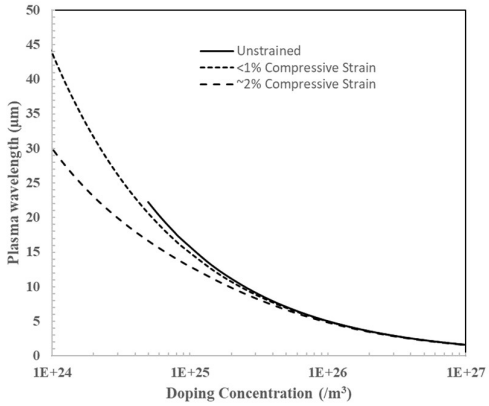

Fig. 3: Variation of plasma frequency with doping concentration for unstrained, and 1% and 2% compressive strain.

The calculated plasma frequencies as a function of doping densities for the unstrained and compressive strains are shown in Fig. 3. Though the curves are widely separated at low doping, all of them merge as doping > 5 x 10^{19} cm^{-3}.

We now calculate the real part of the permittivity of the GeSn layer under 2% compressive strain for doping density of 10^{20} cm^{-3} for different wavelengths. It is interesting to note that the real part starts becoming negative at a wavelength of 3 µm. This indicates that GeSn can indeed support propagating SP waves over the range 3-20 µm [1, 2].

We have similarly calculated the imaginary part of the permittivity. However, due to high mobility of electrons in the Γ valley of GeSn, the values are found to be quite low indicating that the loss suffered by the propagating SP wave is not much significant.

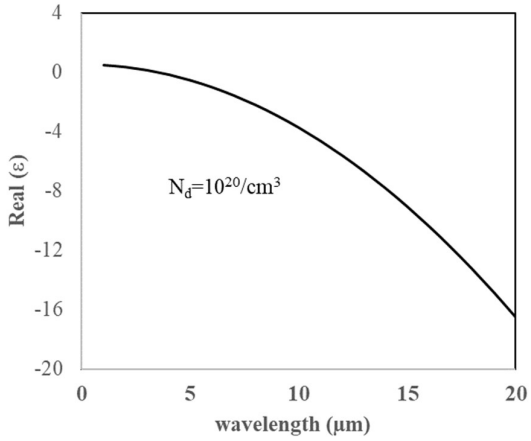

Fig. 4: Variation of real part of permittivity of GeSn alloy with wavelength.

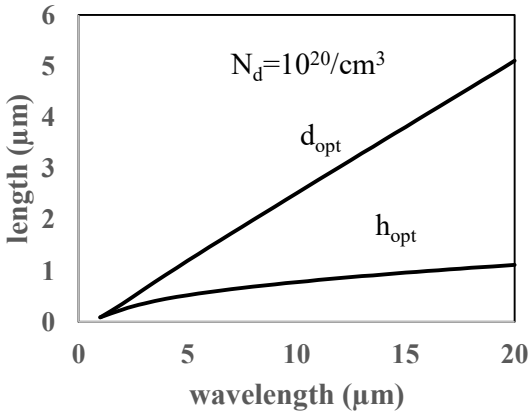

Fig.5: Calculated values of optimized height and period of the grating for different wavelengths for doping density of 10^{20} cm^{-3}

To complete the design of the structure, we now calculate the optimized values of grating height *h* and length *d* as a function of wavelength for the same doping concentration. The values so calculated are shown in Fig. 5. It is to be noted that the length of the grating increases almost linearly with increase in wavelength to satisfy the phase matching condition along the propagation direction.

It is to be noted that in Figs. 3-5, the values for compressively strained GeSn layers are shown. We have obtained similar results for tensile strained and unstrained layers also. The variations are qualitatively the same. It is not possible to include these curves due to limitations of space.

5. Conclusions

We have examined the use of heavily doped GeSn layers as a plasmonic material replacing the highly lossy metals

at IR and MIR ranges. The compositions of GeSn/SiGeSn alloys are chosen to ensure direct gap in GeSn with maximum population in direct Γ valley to minimize loss of SP waves. The calculation indicates the suitability of GeSn as plasmonic layer in the wavelength range 3-20 μm. For excitation of SP waves propagating along length, we have considered GeSn grating and obtained optimum values of height and period length of the grating to ensure efficient coupling between light waves and SP waves. The whole structure may be designed on Si platform to make it CMOS compatible.

6. References

1. Prasanta Kumar Basu, Bratati Mukhopadhyay and Rikmantra Basu, Semiconductor Nanophotonics, Ch. 14, Oxford Univ. Press, Oxford, UK, 2022. ISBN: 9780198784692.

2. S A. Maier (2007) *Plasmonics: Fundamentals and Applications*.Boston, MA: Springer., 2007. ISBN: 978-0387-33150-8

3. M. Cada, D. Blazek, J. Pistora, K. Postava, and P. Siroky (2015) "Theoretical and experimental study of plasmonic effects in heavily doped gallium arsenide and indium phosphide". *Optical Mater Express,* **5**(2) 2015, pp. 340–352. doi:10.1364/OME.5.000340.

4. Y. Zhong, S. D. Malagari, T. Hamilton, and D. Wasserman "Review of mid-infrared plasmonic materials". *Journal of Nanophotonics,* **9**, 2015, pp. 093791(1–21). doi: 10.1117/1.JNP.9.093791

5. R. Soref, J. Hendrickson, and J. W. Cleary, "Mid-to long-wavelength infrared plasmonic-photonics using heavily doped n-Ge/Ge and n-GeSn/ GeSn heterostructures" *Optics Express*, **20**, 4, 2012, pp. 3814-3824. doi: 10.1364/OE.20.003814

6. F. Berkmann et al, Plasmonic gratings from highly doped $Ge_{1-y}Sn_y$ films on Si, *J. Phys. D.: Appl. Phys*. **54**, 445109(9pages), 2021. doi:10.1088/1361-6463/ac1f51.

7. S Wirths, D Buca and S Mantl, "Si-Ge-Sn alloys: from growth to applications," *Prog. Crystal Growth Char Mater*, **62,** 1, 2016, pp. 1-39. doi: 10.1016/j.pcrysgrow.2015.11.001

8. B Mukhopadhyay, G Sen, R Basu, S Mukhopadhyay, and P.K. Basu, "Prediction of large enhancement of electron mobility in direct gap $Ge_{1-x}Sn_x$ alloy," *Phys. Status Solidi B*, **254**, 2017, pp. 1700244. doi: 10.1002/pssb.201700244.

9. S Mukhopadhyay, B Mukhopadhyay, G Sen, and P K Basu, "Maximum theoretical electron mobility in n-type $Ge_{1-x}Sn_x$ due to minimum doping requirement set by intrinsic carrier density", *J. Comp. Electronics* , **20**, 2021, pp. 274-279. doi: 10.1007/s10825-020-01613-3.

10. Bratati Mukhopadhyay, Shyamal Mukhopadhyay and P. K. Basu, "Limitations of Drude Model in Determining Plasma Properties for Multi-valley Semiconductors: A Case Study with $Ge_{1-x}Sn_x$ Alloy", *J of Nanophotonics*, **16**, 2, Apr-Jun 2022, pp 026004 (11 pages). doi: 10.1117/1.JNP.16.026004

11. U. Bog, K. Huska, F. Maerkle, A. N. Mueller, U. Lemmer and T. Mappes, "Design of Plasmonic grating structures towards optimum signal discrimination for biosensing applications", *Optics Express*, **20**, 10 May 2012, pp. .11357-11369 . doi: 10.1364/OE.20.011357.